Simple Preparation of V_2O_5 Nanostructures and Their Characterization

Ch. V. Subba Reddy,[a] Kyung-Il Park, Sun-il Mho,[*] In-Hyeong Yeo,[†] and Su-Moon Park[‡]

Division of Energy Systems Research, Ajou University, Suwon 443-749, Korea. [*]E-mail: mho@ajou.ac.kr
[†]Department of Chemistry, Dongguk University, Seoul 100-715, Korea
[‡]Department of Chemistry and Center for Integrated Molecular Systems, Pohang University of Science and Technology, Pohang 790-784, Korea
Received July 29, 2008

Key Words : Nanomaterials, Vanadium pentoxide, Ammonium vanadates, Cyclic voltammogram

Low-dimensional nanostructures of vanadium oxides and their derivatives have attracted a great deal of interests due to their novel physicochemical properties and potential applications to high-energy lithium batteries, chemical sensors, nanoresonators, and field effect transistors.[1-19] Layer-structured vanadium pentoxide is one of the most studied vanadium oxides despite its low discharge voltages, low electric conductivity, and slow diffusion kinetics of lithium ions.[6-13] In order to improve the performance of lithium batteries by employing vanadium pentoxide as a cathode material, a few methods have been used to prepare vanadium pentoxide with better characteristics, which includes the use of aerogels, xerogels, nanocomposites of LiV_2O_5 with electronically conducting organic polymers and nanostructured materials.[9-12] There have been a few recent attempts to develop synthetic methods for nanomaterials of vanadium oxides but preparation of single-crystal vanadate nanostructures still remains challenging. Generally, nanomaterials are prepared in acidic media[2-5] but very few studies report their synthesis using basic media.[17] Here, we report synthesis of nanosized vanadium oxides by thermal decomposition of ammonium vanadate nanomaterials prepared *via* refluxing and precipitation methods in both basic and acidic media.

Experimental

Nanosized ammonium vanadates (samples 1, 2, and 3) were synthesized from solutions of vanadium pentoxide dissolved in aqueous ammonium solutions using a few different procedures. Sample 1 was synthesized by refluxing a mixed solution of 187 mL of isopropanol and 35 mL of 4.2 M NH_4OH aqueous solution, in which 25 g of V_2O_5 was dissolved. The solution was refluxed in a glass assembly in an oil bath of 70 °C for overnight. The product obtained thereof was then dried in a Petri dish at 60 °C for 48 h. Sample 2 was prepared from a 170 mL of a buffer solution containing 3.53 M NH_4F and 1.73 M NH_3 (pH = 9), in which 9 g of V_2O_5 was dissolved (0.30 M). The solution was stirred for 6 h and then placed in an oven at 90 °C for 5 days for evaporation and crystallization. A dense sol was obtained. Sample 3 was synthesized by precipitating from an acidic ammonium vanadate solution at pH = 2 obtained by adding a concentrated HNO_3 solution to 3 g of V_2O_5 dissolved in a concentrated ammonium buffer solution. The solution was placed in an oven at 90 °C and aged for 5 days. The precipitates thus obtained were filtered, washed with distilled water, and dried at 60 °C for 48 h under static-air conditions. We then obtained nanosized vanadium pentoxide by heating nanosized ammonium vanadates thus obtained at 400 or 600 °C in air.

Crystallographic information was obtained from X-ray diffraction (XRD) data collected over the 2θ range of 2 to 70° by a Rigaku D-max-γA powder diffractometer equipped with Cu Kα radiation (λ = 1.54187 Å). Raman spectra were acquired under ambient conditions by using a Bruker IFS/66 Raman spectrophotometer with an Ar^+ laser operating at 514 nm used as an excitation source. The morphologies of the resulting products were characterized using a FESEM model JSM 6700F field-emission scanning electron microscope. Electrochemical properties of the nanomaterials were investigated in a three-electrode cell with a platinum counter electrode and a silver (Ag) wire pseudo-reference electrode; the working electrode was prepared by first mixing 75% of an active nanostructured material, 20% of carbon black, and 5% of ethylene cellulose and then coating the total mixture of 5.0 mg on the surface of a 1.5 cm^2 ITO glass using a similar technique used for screen printing (V_2O_5 nanomaterial of 2.5 mg/cm^2). A 1.0 M lithium perchlorate solution in propylene carbonate was used as the electrolyte; lithium perchlorate (99.99%, Aldrich) and propylene carbonate (99.7%, Aldrich) were used after recrystallization and distillation, respectively. Cyclic voltammograms (CVs) were recorded at a scan rate of 10 mV/s in a potential limit of −1.0 V and +1.0 V versus a Ag reference electrode using a Zahner IM6 potentiostat/galvanostat.

Results and Discussion

The XRD patterns of the ammonium vanadate and vanadium oxide nanomaterials are shown in Figure 1. All the diffraction peaks of the samples prepared at pH = 9 in the basic solution or by the refluxing method (sample 1 or 2) are indexed to those of $(NH_4)_4V_6O_{17}\cdot 14H_2O$ (JCPDS # 21-0041) (Fig. 1a). The sample prepared from the acidic solution at pH = 2 (sample 3) is believed to be the mixture of

[a]Present address: Department of Chemistry, Southern University and A&M College, Baton Rouge, LA70813, USA.

ammonium vanadate ($NH_4V_3O_8 \cdot 0.5H_2O$) and V_2O_5, as all the diffraction peaks can be indexed to those of ($NH_4V_3O_8 \cdot 0.5H_2O$) (JCPDS # 41-0492) and orthorhombic V_2O_5 (JCPDS # 001-0359) (Fig. 1b). Hydrated ammonium vanadates have two-dimensionally layered structures.[16-19] Ammonium H-bonds contribute to the linkage between the different sheets, as well as the ionic interaction. Water molecules of hydrated ammonium vanadates and of hydrated vanadium pentoxide are also known to exist between the layers.[1-4,16-18] Vanadium in its higher oxidation state is known to exhibit various isopolyvanadates in aqueous solutions at different pH values and concentrations.[20] Vanadium would be in the forms of $V_4O_{12}^{4-}$, $V_2O_7^{4-}$, $V_3O_9^{3-}$, VO_4^{3-}, $VO_3(OH)^{2-}$, and $VO_2(OH)_2^-$ ions in high pH media depending on the extent of hydrolysis forming aquo, hydroxo, or oxo species. By altering reaction conditions such as changes in pH values or concentrations of ammonium ion in the ammonium vanadate aqueous solution, different amounts of ammonium ions and water molecules are incorporated into the crystalline structures. Both high pH values and high NH_4^+ concentrations were shown to lead to the formation of $(NH_4)_4V_6O_{17} \cdot 14H_2O$ in the present study (samples 1 and 2). Acidification of the solution produced a mixture of $NH_4V_3O_8 \cdot 0.5H_2O$ and V_2O_5 (sample 3). The diffraction peaks of the calcinated sample from hydrated ammonium vanadates, *i.e.*, $(NH_4)_4V_6O_{17} \cdot 14H_2O$ (samples 1 and 2: Fig. 1a) and $NH_4V_3O_8 \cdot 0.5H_2O$-V_2O_5 mixture (sample 3: Fig. 1b), are indexed to the orthorhombic structure of V_2O_5 (JCPDS # 001- 0359) (Fig. 1c) upon calcination of sample 1 or 2,

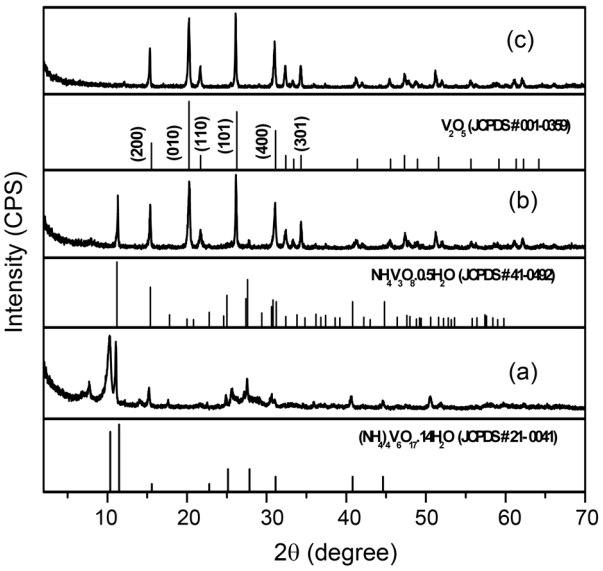

Figure 1. XRD patterns of (a) $(NH_4)_4V_6O_{17} \cdot 14H_2O$ prepared either by evaporation and crystallization from the ammonia/ammonium buffered (pH = 9) vanadate solution (sample 2) or by refluxing from the isopropanol ammonium vanadate aqueous solution (sample 1), (b) the mixture of $NH_4V_3O_8 \cdot 0.5H_2O$ and V_2O_5 prepared by precipitation at pH = 2 from a ammonium vanadate aqueous solution (sample 3), and (c) V_2O_5 formed by calcinations of the hydrated ammonium vanadates at 400 °C or 600 °C (sample 1 and 2). There was no basic difference between samples 1 and 2 in their XRD data.

which must have resulted from the release of NH_3 and H_2O vapor. The conversion of hydrated ammonium vanadates to vanadium pentoxide can be characterized by the frame-work rearrangement of coordination of vanadium atoms as a consequence of release of NH_3 and H_2O.

The Raman spectra of ammonium vanadate [$(NH_4)_4V_6O_{17} \cdot 14H_2O$] (Fig. 2a) and V_2O_5 (Fig. 2b) nanomaterials prepared by the reflux method are shown in Figure 2. In the case of hydrated ammonium vanadate (Fig. 2a), the peaks at 970 cm^{-1} and 998 cm^{-1} are assigned to the V-O stretching motion of tetrahedral and distorted square pyramids, respectively, while the broad band at 680 cm^{-1} is due to the V-O-V stretching mode, and bands below 400 cm^{-1} are from the bending modes of V-O and the lattice modes. According to the reported Raman spectra of vanadium oxides and ammonium vanadates, the Raman bands for V-O and V-O-V stretching modes are observed in the frequency ranges of 800-1000 cm^{-1} and 400-800 cm^{-1}, respectively, while those for the V-O bending and the lattice modes are located below 400 cm^{-1}.[21-23] The Raman spectrum of V_2O_5 prepared in this work is in good agreement with those previously reported.[9,13,22,23] In the Raman spectrum of V_2O_5 (Fig. 2b), the peak at 998 cm^{-1} is assigned to the V-O stretching band of distorted square pyramids, while those at 709, 535, and 489 cm^{-1} are due to the V-O-V stretching modes. There is one V-O stretching peak at 998 cm^{-1} of square pyramids in V_2O_5 (Fig. 2b), compared to the two V-O stretching peaks for tetrahedral and square pyramids in $(NH_4)_4V_6O_{17} \cdot 14H_2O$ (Fig. 2a). The spectral shift observed for the V-O-V stretching mode in V_2O_5 from 680 cm^{-1} for $(NH_4)_4V_6O_{17} \cdot 14H_2O$ (Fig. 2a) to 709 cm^{-1} (Fig. 2b) is due to not only different environments of vanadium and oxygen in the lattices but also the hydrogen bonding caused by ammonium ions and water molecules.

FESEM images of hydrated ammonium vanadate and vanadium pentoxide prepared by the reflux and the precipitation methods in aqueous media containing ammonium ions

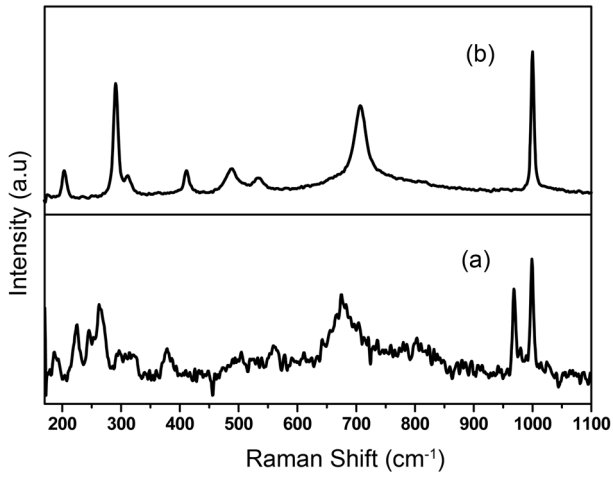

Figure 2. Raman spectra of (a) $(NH_4)_4V_6O_{17} \cdot 14H_2O$ prepared by the reflux method (sample 1), (b) V_2O_5 formed by calcinating sample 1 at 400 °C. Similar spectra were obtained for other samples.

are shown in Figure 3. Shown in Figures 3a are nanodisks of $(NH_4)_4V_6O_{17}\cdot 14H_2O$ prepared by the reflux and evaporation methods (sample 1), while disk- and granule-shaped V_2O_5 obtained upon subsequent calcination of the nanodisks shown in Figure 3a are shown in Figure 3b; both have similar shapes with diameters ranging from 100 to 300 nm and thicknesses of about 60 nm. Figure 3c shows that nanorods and nanobelts of about 200 nm in width and about 10 μm in length were obtained from hydrated ammonium vanadates regardless of whether their components are $(NH_4)_4V_6O_{17}\cdot 14H_2O$ or $NH_4V_3O_8\cdot 0.5H_2O$ when they were prepared by evaporation and crystallization or precipitation from the aqueous ammonium solutions. In other words, samples 2 and 3 were obtained with the morphology shown in Figure 3c. When samples 2 and 3 were calcinated at 400 or 600 °C, the V_2O_5 nanorods and nanobelts shown in Figure 3d were obtained; which had typical lengths of about 10 μm and diameters ranging from 100 to 500 nm.

Our work here demonstrates that one can synthesize large amounts of vanadium oxide nanomaterials at low temperatures without sophisticated equipment and/or elaborate templates or catalysts through cost-effective synthetic procedures. Because the crystal structures of ammonium vanadates and vanadium oxides have two dimensionally layered structures, V_2O_5 nanomaterials grow as belts or rods with the directional growth along a particular axis upon calcination of thus grown vanadates. However, the directional growth in a particular axis was found to be inhibited by continuous disturbance by refluxing the solution, which leads to the round flat disk type of the crystallites. This is, to our knowledge, the first systematic demonstration of formation of various nanostructures of vanadates depending on experimental conditions such as pH of the medium and other reaction conditions. Also, this is the first demonstration that large amounts of nanostructured materials can be prepared without elaborate procedures.

In efforts to evaluate the nanostructured vanadium pentoxide compounds thus prepared, we ran cyclic voltammetric experiments on various forms of nanomaterials. Figure 4 shows cyclic voltammograms (CVs) of three different forms of vanadium pentoxide nanomaterials obtained from their ammonium vanadate precursers prepared by: (a) reflux (nanodisks obtained by calcination of sample 1: Figure 3b), (b) evaporation and crystallization (nanorods/belts obtained by calcination of sample 2, Fig. 3d), and (c) precipitation in the acidic solution (nanorods/belts obtained by calcination of sample 3, Figure 3d). Note that the morphology of the V_2O_5 nanostructures obtained from samples 2 and 3 was about the same as seen from Figure 3d. However, their performances in CVs were significantly different from each other as seen in Figure 4. The CVs obtained from vanadium oxide nanomaterials exhibit broad cathodic and anodic waves, which are attributed to the lithium ion insertion to and desertion from the vanadium oxide electrode materials depending on the valence state of vanadium. The CV shapes are similar to each other and the shapes of cathodic and anodic waves do not severely depend on the morphology of the cathode nanomaterials. However, the electron transfer reaction kinetics for the nanorods/belts electrodes obtained from the precursor prepared in the acidic medium (sample 3: Fig. 4c) is significantly more facile than those for nanodisks obtained from sample 1 (Fig. 4a and b) as can be seen from how fast the current rises as well as peak separations between the anodic and cathodic peaks. It is particularly interesting that the electrode prepared using nanodisks obtained from sample 2 displays the poorest performance of all (Fig. 4b) as

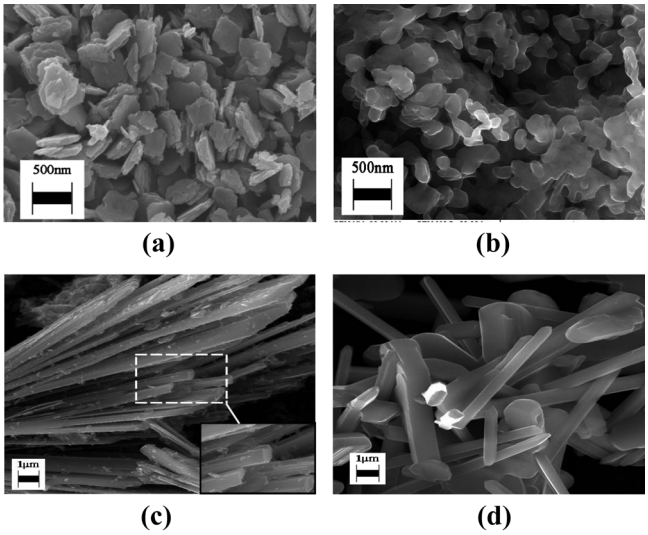

Figure 3. FESEM images of: (a) $(NH_4)_4V_6O_{17}\cdot 14H_2O$ nanodisks prepared by the reflux method (sample 1), (b) V_2O_5 nanodisks and granules formed by calcinating sample 1 at 400 °C, (c) ammonium vanadates (both $(NH_4)_4V_6O_{17}\cdot 14H_2O$ and $NH_4V_3O_8\cdot 0.5H_2O$) nanorods and belts prepared from the aqueous ammonium vanadate solutions by precipitation method (sample 2 and 3), and (d) V_2O_5 nanorods and sheets formed by calcinating samples 2 and 3 at 400 °C.

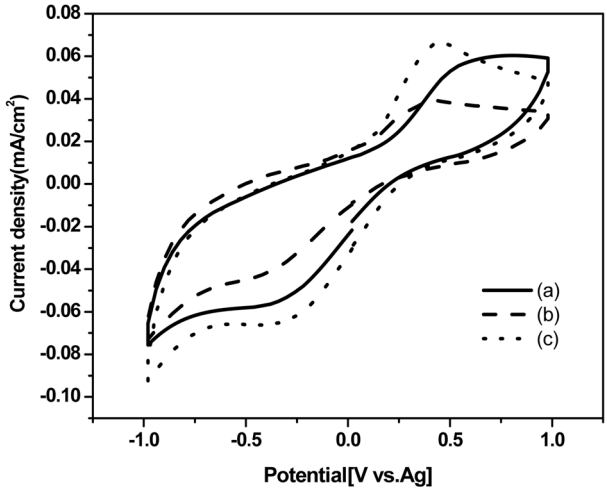

Figure 4. Cyclic voltammograms obtained in a 1 M $LiClO_4$ propylene carbonate solution at a scan rate of 10 mV/s. The working electrodes are composed of the V_2O_5 nanomaterials (75%), carbon (20%), and ethylene cellulose (5%). Film electrodes were prepared to contain the V_2O_5 nanomaterial of 2.5 mg/cm^2. The V_2O_5 nanomaterials are obtained upon calcination (at 400 °C) of: (a) sample 1, (b) sample 2, and (c) sample 3.

judged from the slow rise in currents, the low peak current, and the large peak separation observed during oxidation (de-intercalation) and reduction (intercalation) reactions.

Finally, we have also evaluated the diffusion coefficients of Li^+ during the intercalation reaction by running the peak current dependency on the scan rate (not shown) and obtained average diffusion coefficients ranging from 7.7×10^{-12} for the electrode derived from sample 3 as a precursor, through 5.5×10^{-12} for the electrode obtained from sample 1, to 1.7×10^{-12} cm^2 s^{-1} for the electrode obtained by calcination of sample 2. We believe that the capability of intercalating Li^+ upon reduction of V_2O_5 is determined by the vacant space introduced when the nanostructures prepared in aqueous media are calcinated. The differences shown by the electrodes prepared from these nanostructured precursors appear to depend on the relative amounts of ammonium ions and water molecules in the precursors. While no differences were seen in ammonium ion and water contents in the calcinated samples in their crystal diffraction as well as Raman data, the differences in crystal structures of calcinated nanostructures introduced, albeit small, by the loss of ammonium ions and water molecules might have caused the differences in cyclic voltammetric behaviors.

Conclusions

Nanostructures of V_2O_5 were prepared by thermal decomposition of hydrated ammonium vanadate nanomaterials. The nanosized hydrated ammonium vanadates were prepared in nano-disk shapes by refluxing in a highly concentrated ammonium solution (sample 1), in nano-rod and belt shapes by evaporation and crystallization from a high pH ammonium solution (sample 2), or by a precipitation method lowering the pH of the ammonium solution (sample 3). While the reflux and precipitation methods can be applicable to large scale production of low-dimensional nanostructured vanadium oxides, the performances of electrodes prepared from their calcinated nanostructures differ significantly. Nanosized V_2O_5 nano- disks or rods obtained by calcinating the nanostructures obtained by precipitation in acidic media displayed the best performance for Li^+ intercalation.

Acknowledgments. This research was supported by the Korea Science and Engineering Foundation (KOSEF R01-2007-000-20223-0) and by the Korea Research foundation Grant funded by the Korean Government (MOEHRD KRF-2007-412-J04003). The authors greatly acknowledge valuable contributions by Eun-Ho Lee at the Center for Materials Characterization of Ajou University in the structural analysis using XRD.

References

1. Wang, Y.; Cao, G. *Chem. Mater.* **2006**, *18*, 2787.
2. Liu, J.; Wang, X.; Peng, Q.; Li, Y. *Adv. Mater.* **2005**, *17*, 764.
3. Pdtkov, V.; Trikalitis, P. N.; Bozin, E. S.; Billinge, S. J. L.; Vogt, T.; Kanatzidis, M. G. *J. Am. Chem. Soc.* **2002**, *124*, 10157.
4. Yao, T.; Oka, Y.; Yamamoto, N. *Mater. Res. Bull.* **1992**, *27*, 669.
5. Kannan, A. M.; Manthiram, A. *Solid State Ionics* **2003**, *159*, 265.
6. Chew, S. Y.; Feng, C. S.; Ng, H.; Wang, J.; Guo, A.; Liu, H. *J. Electrochem. Soc.* **2007**, *154*, A633.
7. Doh, C.-H.; Kim, S. I.; Jeong, K.-Y.; Jin, B.-S.; An, K. H.; Min, B. C.; Moon, S.-I.; Yun, M.-S. *Bull. Korean Chem. Soc.* **2006**, *27*, 1175.
8. Park, Y. J.; Lee, J. W.; Lee, Y.-G.; Kim, K. M.; Kang, M. G.; Lee, Y. *Bull. Korean Chem. Soc.* **2007**, *28*, 2226.
9. Subba Reddy, Ch. V.; Wei, J.; Yao, Z. Q.; Rong, D. Z.; Chen, W.; Mho, S.-I.; Kalluru, R. R. *J. Power Sources* **2007**, *166*, 244.
10. Qiao, H.; Zhu, X.; Zheng, Z.; Liu, L.; Zhang, L. *Electrochem. Commun.* **2006**, *8*, 21.
11. Huguenin, F.; Torresi, R. M.; Buttry, D. A. *J. Electrochem. Soc.* **2002**, *149*, A546.
12. Coustier, F.; Hill, J.; Owens, B. B.; Passerini, S.; Smyrl, W. H. *J. Electrochem. Soc.* **1999**, *146*, 1355.
13. Balog, P.; Orosel, D.; Cancarevic, Z.; Schoen, C.; Jansen, M. *J. Alloys Compd.* **2007**, *29*, 87.
14. Patrisi, C. J.; Martin, C. R. *J. Electrochem. Soc.* **2001**, *148*, A1247.
15. Kam, K. C.; Cheetham, A. K. *Mater. Res. Bull.* **2006**, *41*, 1015.
16. Lampe-Onnerud, C.; Thomas, J. O. *J. Mater. Chem.* **1995**, *5*, 1075.
17. Ren, T.-Z.; Yuan, A.-Y.; Zou, X. *Cryst. Res. Technol.* **2007**, *42*, 317.
18. Theobald, F. R.; Theobald, J. G.; Vedrine, J. C.; Clad, R.; Renard, J. *J. Phys. Chem. Solids* **1984**, *45*, 581.
19. Kong, L.; Liu, Z.; Shao, M.; Xie, Q.; Yu, W.; Qian, Y. *J. Solid State Chem.* **2004**, *177*, 690.
20. Livage, J. *Coord. Chem. Rev.* **1998**, *999*, 178.
21. Mai, L. Q.; Lao, C. S.; Hu, B.; Zhou, J.; Qi, Y. Y.; Chen, W.; Gu, E. D.; Wang, Z. L. *J. Phys. Chem.* **2006**, *B 110*, 18138.
22. Twu, J.; Shih, C. F.; Guo, T. H.; Chen, K. H. *J. Mater. Chem.* **1997**, *7*, 2273.
23. Hardcastle, F. D.; Wach, I. E. *J. Phys. Chem.* **1991**, *95*, 5031.